UDC 539.4

Surface Strengthening Behavior of Magnesium Alloy with Laser Thermal Loading under Rapid Cooling

Y. Q. Ge,[a,1] X. Chen,[a] W. X. Wang,[b] and S. Guo[b]

[a] College of Materials Science and Engineering, Taiyuan University of Science and Technology, Taiyuan City, Shanxi Province, China

[b] College of Materials Science and Engineering, Taiyuan University of Technology, Taiyuan City, Shanxi Province, China

[1] geyaqiong@tyust.edu.cn

УДК 539.4

Поверхностное упрочнение магниевого сплава путем лазерной термообработки в условиях быстрого охлаждения

Я. К. Ге[а], К. Чен[а], В. К. Ванг[б], С. Гуо[б]

[а] Колледж материаловедения и инжиниринга, Тайюаньский университет науки и техники, Тайюань, провинция Шаньси, Китай

[б] Колледж материаловедения и инжиниринга, Тайюаньский технологический университет, Тайюань, провинция Шаньси, Китай

Выполнено лазерное поверхностное упрочнение образца из магниевого сплава AZ31B с его одновременным быстрым охлаждением в жидком азоте. Исследованы характер и механизм поверхностного упрочнения. Благодаря механизмам уменьшения размеров зерен и возникновения твердого суперрасплава, а также их влиянию на движение дислокаций и образование аморфной структуры имеет место значительное повышение микротвердости, износостойкости и вязкости разрушения магниевого сплава. Ускоренные режимы нагрева лазером и охлаждения в жидком азоте способствовали уменьшению размеров зерен в упрочненном поверхностном слое и формированию аморфной структуры. Большинство дислокаций было обнаружено в упрочненном слое, а не в подложке. Искажение кристаллической решетки, вызванное высокой концентрацией алюминия, растворенного в α-Mg фазе, также повышает устойчивость данного сплава к движению дислокаций.

Ключевые слова: магниевый сплав, лазерное поверхностное упрочнение, механизм упрочнения, быстрое охлаждение, движение дислокаций.

Introduction. With the rapid development of modern science and technology, magnesium alloy plays an increasing important role in science development and industrial application because of their advantages of low density, high specific strength and good elastic modulus, and so on [1]. But there are still some weaknesses of magnesium alloy material, such as poor hardness, wear resistance and fracture toughness, limited its wider application and development [2].

The main forms of metal failure are fracture, corrosion and wear, which begin from the material's surface in many cases. Therefore, according to the relationship of material's composition, microstructure and performance, the comprehensive performance of magnesium alloy could be strengthened by surface modifying, without changing the original characteristics of magnesium alloy except the modified zone [3].

© Y. Q. GE, X. CHEN, W. X. WANG, S. GUO, 2018

There are lots of surface modifying strategies of magnesium alloys [4]. Laser surface strengthening is a more effective method in all surface treatments. It is a well known technique for the surface strengthening because of rapid heating and cooling rate and simple process [5]. Many previous studies focused on the effects of laser surface strengthening on steels and some light alloys [6, 7]. However, the effects of laser surface strengthening on magnesium alloys are relatively less studied. Therefore, it is essential to further the laser surface strengthening technique on magnesium alloys. As is known, with more rapid cooling rate, some especial rapid solidification microstructure may be obtained [8]. Nevertheless, previous laser surface strengthening studies were carried out in air-cooling condition [9, 10]. There are few researches to increase the cooling rate and to obtain better performance.

In this work we show a new approach for the laser surface strengthening technique in which the main idea of rapid cooling is used. The surface of magnesium alloy was heated by laser, while the samples were extremely rapidly cooled in liquid nitrogen. We conduct this study to strength the surface performance of magnesium alloy and to discuss the surface strengthening mechanism.

1. **Experimental**.

1.1. ***Experimental Materials***. In the present investigation, a hot-rolling AZ31B magnesium alloy with a composition (wt.%) of 3.22 Al, 1.15 Zn, 0.4 Mn, 0.0133 Si, 0.0019 Fe and Mg-balance, was chosen as the substrate material. All samples were cut into coupons with a dimension of 180×75×10 mm by means of wire electrical discharge machining.

1.2. ***Preprocessing***. To improve the absorptive capacity of magnesium alloy's surface to laser, the surface of the magnesium alloy was pretreated. Firstly, the specimens were ground with No. 80 abrasive papers, cleaned by acetone, and then air-dried. After that, special light-absorbing paint was evenly sprayed to the treated surface, and then air-dried again. Table 1 lists the paint components.

A 5 kW CO_2 laser (HUST-JKT5170) connected to a computer for numerical controlling was used. The laser melting process under liquid nitrogen cooling condition is shown in Figs. 1 and 2. The liquid level of liquid nitrogen should be observed all the time, and liquid nitrogen and argon should be added constantly to ensure liquid nitrogen and magnesium alloy's surface was at the same level. The laser surface melting parameters are listed in Table 2.

T a b l e 1

Chemical Compositions of Light Absorption Coating and AZ31B Magnesium

Element	C	O	Ca	Zr	Sn	Sb	Other	Total
Weight (%)	5.21	21.81	35.39	1.00	3.70	24.40	8.48	100.00
Atomic (%)	14.51	45.60	29.54	0.37	1.04	6.70	2.24	100.00

T a b l e 2

Laser Surface Heating Parameters

Laser power P (kW)	Scanning speed v, mm/min	Sport diameter D, mm	Shielding gas flow Q, l/min
2500	600	5	15

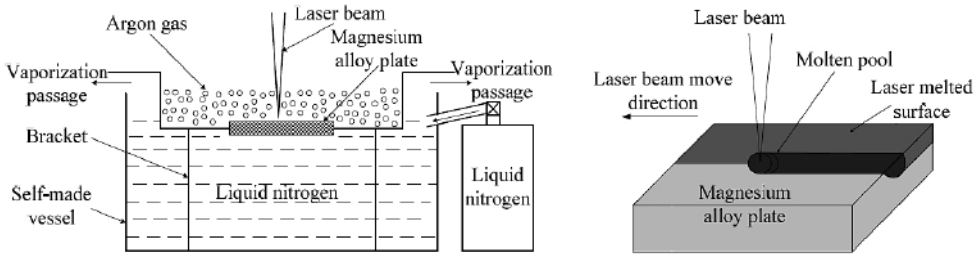

Fig. 1. Laser surface strengthening under liquid nitrogen cooling condition: (a) sketch map of liquid nitrogen cooling condition; (b) sketch map of laser surface strengthening.

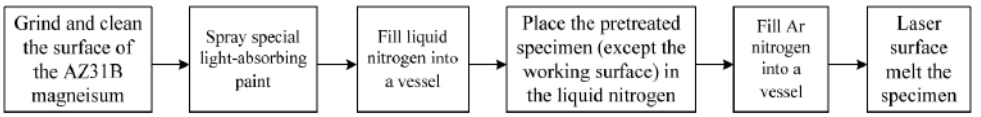

Fig. 2. Laser surface strengthening process.

1.3. ***Characterization***. Microstructure and phase constituents were examined by the optical microscope (CMM-20), the scanning electron microscope (JSM-6700F), the high resolution transmission electron microscopy (JEM-2100F) and the X-ray diffractometer (Y-2000). Wearing resistance was measured by the reciprocating abrasion machine (MFT-R4000), and the specimen was fixed on the horizontal workbench and was worn out with the horizontal movement of the workbench under the GCr15 counter wearing specimen and 500 g load, 20 min fraction time and 100 rpm rotational speed. Pendulum impact testing machine was used for impact study with impact energy of 4.8 J and testing temperature of 20℃, and the specimen dimensions are shown in Fig. 3.

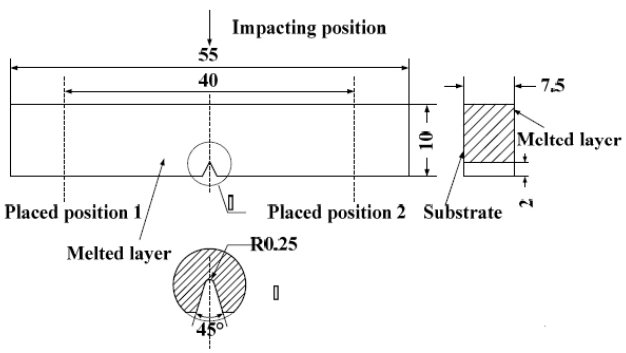

Fig. 3. V-type notch impact specimen (unit: mm).

2. **Results**.

2.1. ***Morphology of the Strengthening Zone***. As shown in Fig. 4, the surface of the strengthening zone appeared uneven. During the laser surface strengthening, when the part of laser energy absorbed by the surface of magnesium alloy heated it beyond its boiling point of 1090℃, the surface of magnesium alloy would vaporized. The recoil of the magnesium alloy vapor would produce some pressure which could result in the formation of the uneven surface. As a result of the laser heat source of the Gauss mode, the strengthening layer exhibited the crescent-shaped morphology as shown in Fig. 5. The depth of the strengthening zone was about 230 μm.

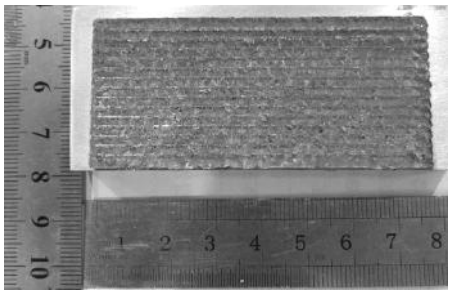

Fig. 4. Macroscopic morphology of the strengthening zone.

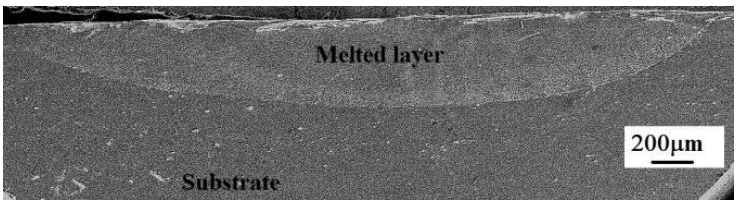

Fig. 5. Cross-sectional macrograph of the strengthening layer.

2.2. ***Surface Strength Behavior***. Figure 6 shows the microhardness of the strengthening layer by laser thermal loading. It revealed that microhardness of strengthening layer (about 150.3 HV) cooled under rapid cooling condition has significantly increased by about 3 times as compared to that of substrate (about 50 HV).

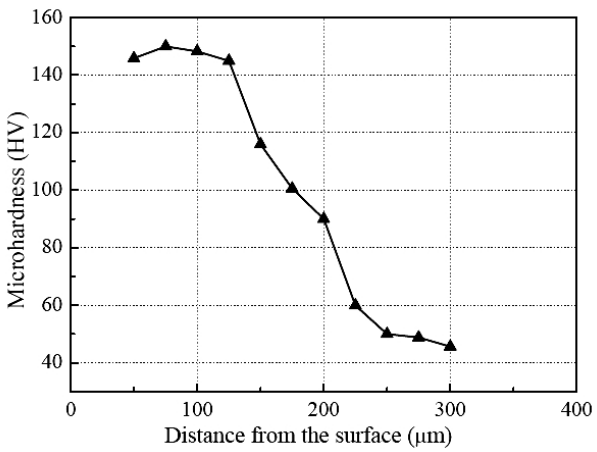

Fig. 6. Microhardness of strengthening layer.

Observed from the morphology of the worn surface (Fig. 7a and 7b), both of the as-received magnesium alloy and the strengthening layer exhibited the characteristics of abrasive wear. The wear width of them was 990 and 880 μm, respectively. There were groove and abrasive dust on the abrasive surface of both of them, but some zones of as-received magnesium alloy peeled off, as shown in Fig. 7c and 7d. Apparent oxide even appeared on the peeling area. But there was almost no oxidative cracking, and the groove and abrasive dust were still the typical wear morphology of the strengthening layer. The wear data of substrate and the strengthening layer are listed in Table 3. This implies that the wear performance of magnesium alloy could be improved by laser thermal strengthening.

T a b l e 3

Wear Data of the Substrate and Strengthening Layer

Characteristic	As-received magnesium alloy	The strengthening layer
Wear loss (mg)	10	5
The maximum friction coefficient	0.961	0.261
The average friction coefficient	0.578	0.168
The maximum microhardness (HV)	50.0	150.3
The grain size (μm)	58.7	5.1

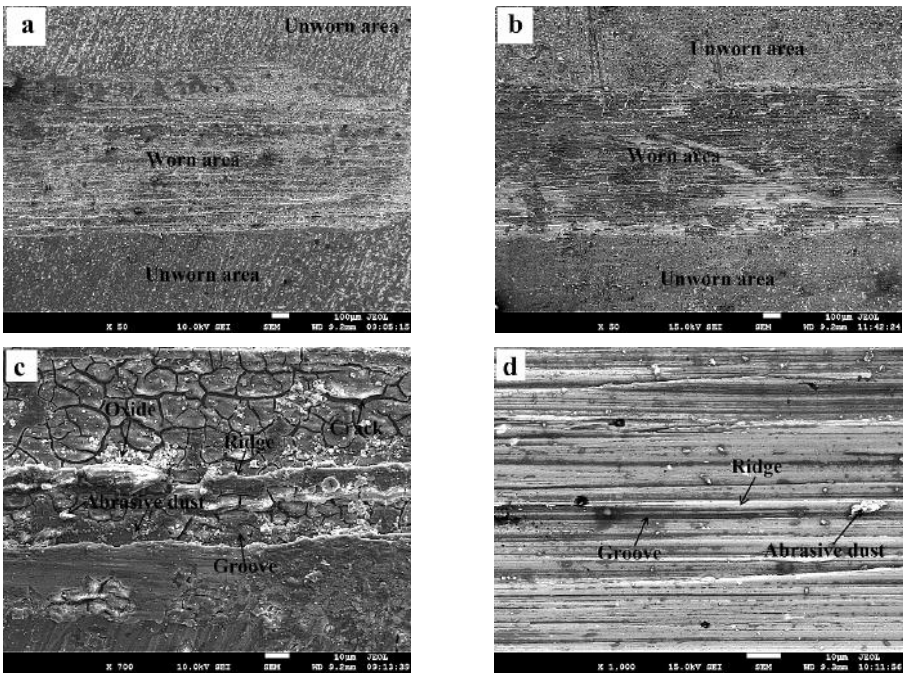

Fig. 7. Wear morphology: (a) as-received magnesium alloy; (b) the strengthening layer; (c) magnified figure a; (d) magnified figure c.

Figure 8 depicts the fracture surface of the laser melted layer at room temperature after sharply impact test. The melted layer exhibited ductile dimple fracture in combination with cleavage fracture and a little plastic deformation (Fig. 8b), because there were some features dimples. But the substrate (Fig. 8c) displayed brittle fracture with sensible cleavage steps and cracks.

3. **Discussion**. The average grain size of the original magnesium alloy and strengthening layer was about 58.7 and 5.1 μm. From the bottom (Fig. 9a) to the top (Fig. 9d) of the strengthening layer, the solidification rate of the melt gradually increased, the grain size gradually decreased, and in the upper zone (Fig. 9c and 9d) the grain refined remarkably. Under the extremely low temperature cooling of liquid nitrogen, the heat transferring speed of melt was greatly improved, but this also improved the solidification cooling rate dramatically. So did the undercooling. With such a high degree of undercooling, nucleation and growth were inhibited, the strengthening layer showed a high degree of grain refinement. Especially, the grains in the upper region of the strengthening layer were more uniform. The strong convection of the molten pool made the edge of the original

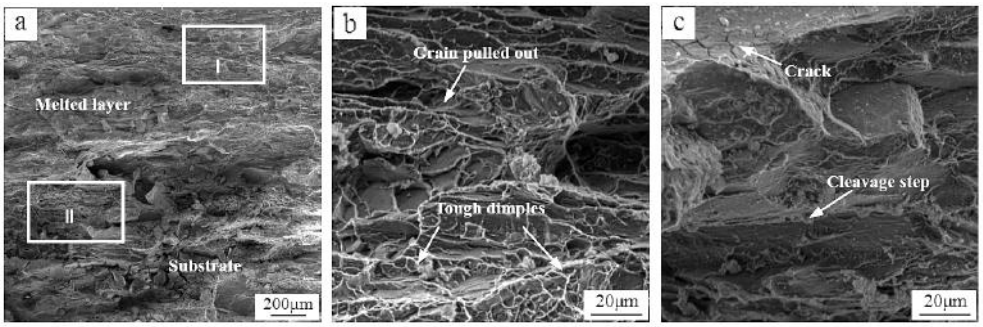

Fig. 8. Impact fracture of strengthening layer: (a) morphology of impact fracture; (b) magnified view of *I* region; (c) magnified view of *II* region.

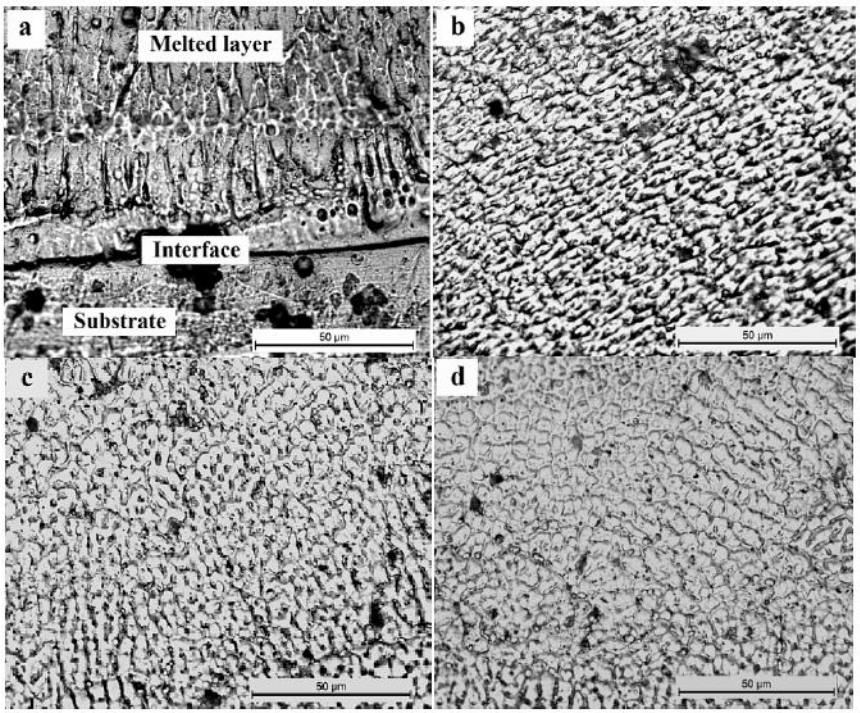

Fig. 9. Microstructure of the melted layer: (a) interface between strengthening layer and substrate; (b) bottom of strengthening layer; (c) middle of strengthening layer; (d) upper part of strengthening layer.

structures in the middle and upper part broken, and these broken fragments were dispersed into the molted pool and became the core of the new structure. And heterogeneous nucleation was occurred at the free surface of the molten pool. Moreover, the cooling rate of the melt was improved under liquid nitrogen cooling circumstance, while cooling rate of the middle and the upper regions of the melt were rapider which could inhibit the crystal nucleus grew. Thus, there were more crystal nucleus in the upper region, and the growth of the crystal nucleus was inhibited.

After laser surface heating and melting on magnesium alloy under rapid cooling condition, the dislocation density greatly increased, as is shown in Fig. 10. Compared with the matrix, the dislocation density greatly increased at the grain boundaries, and dislocation tangling even appeared. In addition, there were also more dislocations inside the grains.

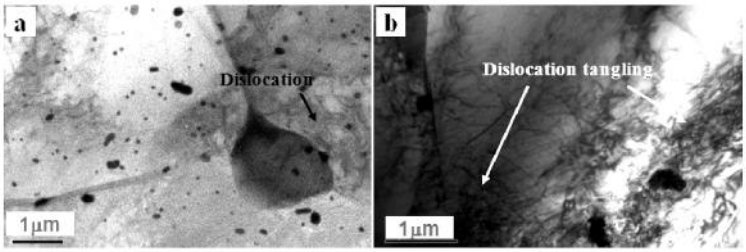

Fig. 10. Dislocations in (a) as-received magnesium alloy and (b) the strengthening layer.

On the one hand, there were more grain boundaries caused by the grain refinement, and they could hinder the movement of dislocations, so a large number of dislocations tangled at the interface. On the other hand, plastic deformation caused by thermal stress during laser heating and rapid cooling was also an important reason of the increase of dislocation density. The thermal stress was simulated by ANSYS. Ultimately, there was tension stress in strengthening layer and compressive stress in substrate, and the maximum tension stress was in the upper part of the strengthening layer with the value of 111 MPa. By the influence of the uneven temperature field, the thermal stress in the strengthening layer was also uniform. In the cooling process, the melts in the bottom of the melted pool was cooled down firstly and began to shrink, meanwhile the substrate restricted its shrink. Therefore, there was tension stress in this firstly solidify region, and the substrate was subjected to compressive stress. With the continued cooling, the middle and the upper parts of the melted cooled down to produce tensile stresses.

There were some regions, in which the atoms arranged randomly as is shown in Fig. 11, and another typical feature was there was an obvious boundary between atom-cluttered area and the well-ordered atomic region. It indicated that non-crystallization appeared in the strengthening layer. It also showed that laser surface strengthening on magnesium alloy under liquid nitrogen cooling environment could realize amorphization in local areas on the surface of magnesium alloy.

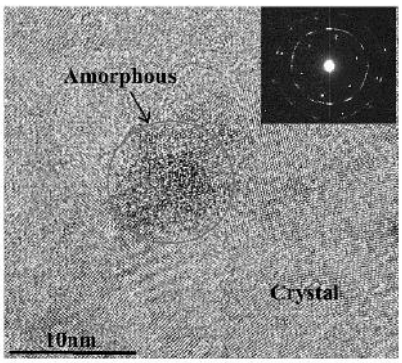

Fig. 11. Amorphous regions in the strengthening layer.

However, the amorphized region was not as uniform as it was imagined, and crystalline and amorphous region alternately appeared in melted layer. Laser surface strengthening was a rapid heating and cooling process, so magnesium alloy melt's residence time in liquid was short. Furthermore, laser surface strengthening under liquid nitrogen cooling condition would be affected by the extremely low temperature of liquid nitrogen, so the cooling rate of magnesium alloy melt would be further accelerated. It led to a shorter liquid stay and heterogeneous components. Moreover, epitaxial growth of

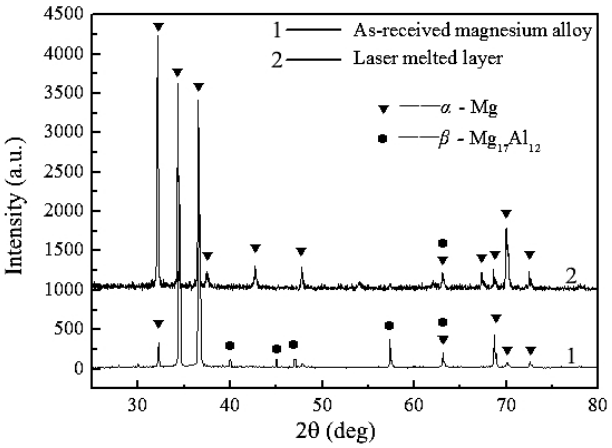

Fig. 12. X-ray diffraction patterns of as-received magnesium alloy and the melted layer.

solidification structure would increase the critical cooling rate R_c, thereby the amorphous forming ability would be reduced. In addition, if there were refractory particles which could create structure fluctuation condition for heterogeneous nucleation, the amorphous formation ability would also be reduced.

The phases of as-received magnesium alloy and the strengthening layer were showed in Fig. 12. The as-received magnesium alloy which was formed near equilibrium state was mainly composed of α-Mg and β-$Mg_{17}Al_{12}$. According to the theory of phases' semi quantitative analysis, β in the strengthening layer was poor, and the diffraction peaks was a little leftward. During the laser strengthening under liquid nitrogen cooling condition, owing to rapider cooling rate and non-equilibrium solidification, the interface of solid and liquid moved fast, so some elements which hadn't diffused were solute in the interface and solidified. As a result, the eutectic transformation of $L \rightarrow \alpha$-Mg+β-$Mg_{17}Al_{12}$ occurred under the equilibrium state was inhibited, and the content of β-$Mg_{17}Al_{12}$ was little. Many researches had proved that[11], on the condition of rapid solidification, some elements of which the atomic radius were in the range of $\pm 15\%$ would be solute into α-Mg. And the reason of diffraction peak shifting was also mainly due to the increase of solid solubility and the grain refinement under this rapid cooling condition. These illustrated that in the strengthening layer large numbers of Al element dissolved into α-Mg, and it could introduce distortion of lattice. This may increase the resistance to the dislocation motion.

Conclusions

1. Due to laser heating and rapid cooling, a strengthening zone with the depth of about 230 μm was obtained.

2. Microhardness of strengthening layer had significantly increased by about 3 times. Wear resistance of the strengthening layer was improved obviously. But there was almost no oxidative cracking in the strengthening layer. And the maximum and average friction coefficient of the strengthening layer was 0.261 and 0.168 which was less than it of the original material. There was some feature of dimples in the strengthening layer.

3. The microstructure of the strengthening layer was greatly refined. The average grain size of the original magnesium alloy and strengthening layer was about 58.7 and 5.1 μm. Owing to rapid cooling, the dislocations in the strengthening layer were increased comparing to the as-received magnesium alloy, and some area with the feature of amorphous structure was formed. Compared with as-received magnesium alloy, the strengthening layer was almost composed of α-Mg, but β-$Mg_{17}Al_{12}$ was few.

Acknowledgments. This project is supported by National Natural Science Foundation of China (Grant No. 51405324), Natural Science Foundation for Youths of Shanxi Province (Grant No. 201701D221068), Fund for Shanxi Key Subjects Construction, PhD research startup foundation of TYUST University (Grant No. 20152010).

Р е з ю м е

Виконано лазерне поверхневе зміцнення зразка з магнієвого сплаву AZ31B з його одночасним швидким охолодженням у рідкому азоті. Досліджено характер і механізми поверхневого зміцнення. Завдяки механізмам зменшення розмірів зерен і виникнення твердого суперрозплаву та їх впливу на рух дислокацій і виникнення аморфної структури має місце значне підвищення мікротвердості, зносостійкості і в'язкості руйнування магнієвого сплаву. Прискорені режими нагрівання лазером і охолодження у рідкому азоті сприяли зменшенню розмірів зерен у зміцненому поверхневому шарі і формуванню аморфної структури. Більшість дислокацій було виявлено у зміцненому шарі, а не в підкладці. Спотворення кристалічної решітки в результаті високої концентрації алюмінію, що розчиняється в α-Mg фазі, також збільшує стійкість даного сплаву до руху дислокацій.

1. Y. C. Guan, W. Zhou, Z. L. Li, and H. Y. Zheng, "Laser-induced microstructural development and phase evolution in magnesium alloy," *J. Alloy. Compd.*, **582**, 491–495 (2014).
2. Y. Ali, D. Qiu, B. Jiang, et al., "Current research progress in grain refinement of cast magnesium alloys: a review article," *J. Alloy. Compd.*, **619**, 639–651 (2015).
3. C. Taltavull, A. J. López, B. Torres, and J. Rams, "Dry sliding wear behaviour of laser surface melting treated AM60B magnesium alloy," *Surf. Coat. Tech*., **236**, 368–379 (2013).
4. A. Singh and S. P. Harimkar, "Laser surface engineering of magnesium alloys: a review," *JOM*, **64**, No. 6, 716–733 (2012).
5. Z. T. Wang, X. Lin, Y. Q. Cao, and W. D. Huang, "Microstructure evolution in laser surface remelting of Ni–33 wt.%Sn alloy," *J. Alloy. Compd.*, **577**, 309–314 (2013).
6. Y. Lv, "Influence of laser surface melting on the micropitting performance of 35CrMo structural steel gears," *Mater. Sci. Eng. A*, **564**, 1–7 (2013).
7. T. Marcu, M. Todea, I. Gligor, et al., "Effect of surface conditioning on the flowability of Ti6Al7Nb powder for selective laser melting applications," *Appl. Surf. Sci.*, **258**, No. 7, 3276–3282 (2012).
8. D. Lussana, A. Castelero, M. Vedani, et al., "Microstructure refinement and hardening of Ag–20 wt.% Cu alloy by rapid solidification," *J. Alloy. Compd.*, **615**, S633–S637 (2014).
9. A .D. Danikiewice, T. Tanski, and J. D. Dubiel, "Unique properties, development perspectives and expected applications of laser treated casting magnesium alloys," *Arch. Civ. Mech. Eng*., **12**, 318–326 (2012).
10. G. Rapheal, S. Kumar, C. Blawert, and Narendra B. Dahotre, "Wear behavior of plasma electrolytic oxidation (PEO) and hybrid coatings of PEO and laser on MRI 230D magnesium alloy," *Wear*, **271**, 1987–1997 (2011).
11. G. Abbas, L. Li, U. Ghazanfar, and Z. Liu, "Effect of high power diode laser surface melting on wear resistance of magnesium alloys," *Wear*, **260**, 175–180 (2006).

Received 15. 09. 2017